Droplet Formation and Dropping Position Control in Electrostatic Inkjet Phenomena

Shinjiro Umezu, Hodaka Suzuki and Hiroyuki Kawamoto, Department of Mechanical Engineering, Waseda University, Shinjuku, Tokyo, Japan

Abstract

A preliminary investigation was conducted on formation and control of micro droplet in electrostatic inkjet phenomena. High voltage was applied between an insulative capillary tube filled with ion-conductive water and a plate electrode. At the beginning of corona discharge, a Taylor cone was formed at the tip of the tube and the top of the cone was broken to form a very small droplet that was dispersed like mist at wide angle due to the Coulomb repulsive force of charged mist. When the applied voltage was further increased, water droplet was formed periodically. The charge to mass ratio of the droplet was measured and compared with the Rayleigh's limit. It was less than the limit because the droplet vibrated at the formation of the droplet. Another experimental set-up was constructed to control the dropping position of the droplet. A ring electrode was settled between the capillary tube and the plate electrode to control the dropping position of the droplet.

Introduction

It is well known that an electrostatic ink jet phenomenon is observed when a tube filled with ink is used for the pin electrode in a pin-to-plate system.[1] This phenomenon is expected to be applied not only for ink jet printing systems[2] but also for biological and analytical chemistry. This ink jet phenomenon and its application have been investigated by many investigators[3-6] since the first work by Rayleigh[7] on the stability of a charged drop. He deduced that there is a limit to the charge that can be sustained by the drop, above which it becomes unstable and disrupts. This limit is known as the Rayleigh's limit. A number of workers have investigated the effect of an electrostatic field at a liquid surface since then. In any published study, however, nothing has been reported on the relationship between the electrospraying phenomena and the mode of gas discharge, in spite of the fact that kinetics of dark discharge are quite different to those of corona discharge in a pin to plate gas discharge system.[8]

In this paper, we clarify how the formation of the droplet in the corona discharge field is influenced by the mode of discharge, by use of kinetics in the pin-to-plate gas discharge field. In this system droplet was dispersed like mist because of repulsion of charged droplets. We constructed an experimental set-up to bundle the dispersed droplet.

Droplet Formation

Experimental Set-up

An experimental set-up illustrated in Fig. 1 was constructed to investigate characteristics of the formation of droplets in the electrostatic field. The capillary tube made of silica coated by polyimide (Polymicro Technologies, Phoenix, AZ) was equipped with a bottom of a syringe. The tube had 100 μm inner and 170 μm outer diameters. This tube with water was mounted perpendicular to a plate electrode made of stainless steel. DC voltage was applied by a function generator (Iwatsu, Tokyo, SG-4105) and a high voltage amplifier (Matsusada Precision Inc, HEOP-10B2). The current was measured by the voltage drop in a current-shunt resistor. The formation of the droplet was observed with a high-speed microscope camera (Photron Inc., Japan, FASTCAM-MAX 120K model 1) and a light (San-ei Electric Inc., Japan, XEF-501S). Another experimental set-up, shown in Fig. 2 was constructed to measure the charge on an individual droplet. A small hole, 5 mm in diameter, was opened at the center of the plate electrode and parallel plate electrodes were set under the plate electrode. In this configuration, the charged droplet was moved when voltage was applied between the parallel electrodes.

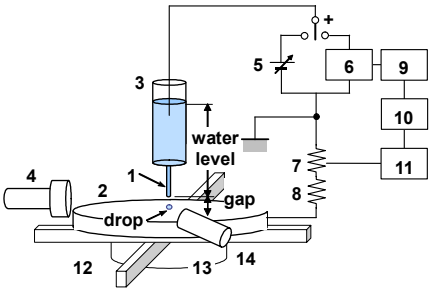

Figure 1. Experimental set-up. (1: water pin electrode, insulative capillary tube filled with water, 2: metal plate electrode, 3: water tank, 4: CCD camera, 5: DC high voltage power supply, 6: high voltage amplifier, 7: shunt resistor, 400 kΩ, 8: resistor: 400 kΩ, 9: function generator, 10: oscilloscope, 11: volt meter, 12: linear stages, x and y directions, 13: mechanical z-stage, 14: stroboscope light)

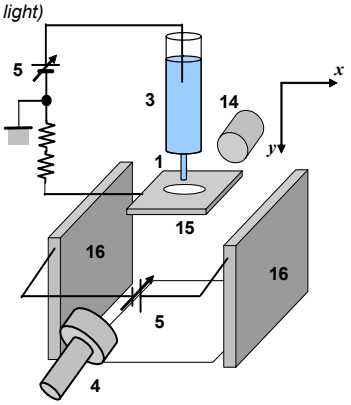

Figure 2. Experimental set-up to measure charge of droplet. (15: metal plate electrode with a hole, 16: parallel plate electrode)

Fundamental Characteristics

In the first place, the current-voltage characteristics of the water pin electrode were measured and compared with those of the metal pin electrode of the same diameter as the inner diameter of the insulating tube. The results are shown in Fig. 3. In case of the water pin electrode, although a pulse current was superposed on the corona current, corresponding to the separation of the droplet, as described below, a stable corona current was measured. Corona current of the water electrode agreed well with that of the metal pin electrode and fundamental characteristics of the discharge were common. That is, no current flowed in the dark discharge region, however, when the applied voltage reached a threshold (about 2 kV), corona discharge took place, and the corona current in the order of micro ampere flowed.

As added in Fig. 3 the formation of the droplet was classified into the following three modes corresponding to the discharge modes.

MODE 1: In the dark discharge region, 0 ~ 2 kV, a drop was formed at the tip of the tube. This became gradually large and finally separated. The diameter of the drop was several times larger than that of the tube diameter and the drop period was long, more than a second. Characteristics and mechanism of MODE 1 were already reported.[6]

MODE 2: At the beginning of the corona discharge, 2 ~ 4 kV, a Taylor cone was formed at the end of the tube and the tip of the cone periodically separated from the cone to form a very small droplet of the order of several tens of microns in diameter. Figure 4 shows the transient formation of droplets in the MODE 2 region. Droplets dispersed over a wide angle, like mist. Trajectory of the droplet was unstable and the frequency of the droplet formation was very high, in the order of kHz.

MODE 3: At higher voltage, the Taylor cone changed to hemispherical and the droplet became relatively large, nearly the same as the tube diameter. Figure 5 shows the formation of the droplet in the MODE 3 region. The frequency of the droplet formation was 10 ~ 100 Hz.

Figure 6 shows the diameter of the droplet. Droplets at MODE 2 were much smaller than those of MODE 1, because only the tip of Taylor cone formed a droplet at MODE 2. The diameter became large at high voltage. There are two possible reasons of this characteristic: one is that the reaction force of the ionic wind prevented the separation of the droplet from the tip of the Taylor cone, and another is relaxation of the electric field, which made the tip of the Taylor cone relatively round. Further investigation is necessary on the mechanism of the droplet formation in the MODE 2 region, for it is anticipated that MODE 2 may be utilized for a micromist spray and formation of the small droplets.

Diameter and Charge of Droplet

A trajectory of a charged droplet was deflected in the electrostatic field formed by the apparatus shown in Fig. 2. Equations of motion of droplet were expressed as follows.

$$m\ddot{x} + c\dot{x} = qE_x \tag{1}$$

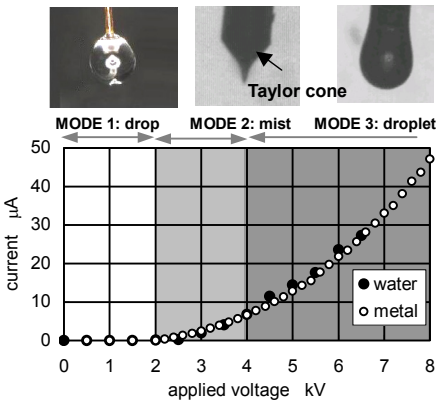

Figure 3. V-I curves in pin-to-plate electrode system. (ϕ 100 μm inner tube diameter, ϕ 100 μm metal pin diameter, 3 mm air gap)

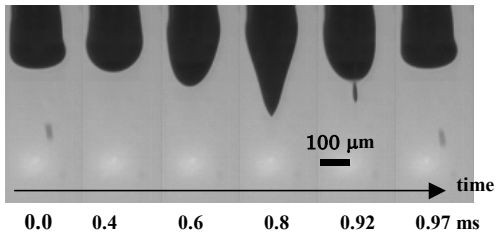

Figure 4. Formation of Taylor cone and droplet at MODE 2. (2.71 kV applied voltage)

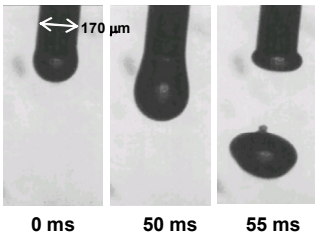

Figure 5. Formation of droplet at MODE 3. (3 mm gap, 70 mm water level, 4.5 kV applied voltage)

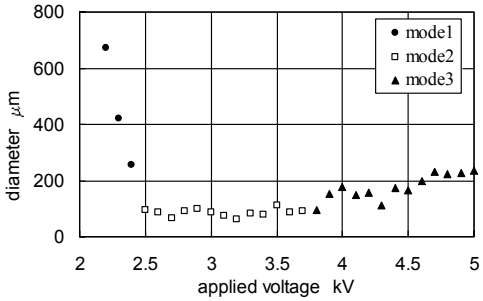

Figure 6. Applied voltage versus droplet diameter.

$$m\ddot{y} + c\dot{y} = mg + qE_y \tag{2}$$

$$c = 6\pi\eta_a r \tag{3}$$

where m is mass of the droplet, c is coefficient of air drag, q is charge of droplet, η_a is viscosity coefficient of air. Mass of droplet

was calculated from the diameter measured by the high speed camera. Figure 7 shows the electric field which was calculated with the Poisson's equation and the conservation of charge. Charge of droplet was calculated from the dropped position and electrostatic field.

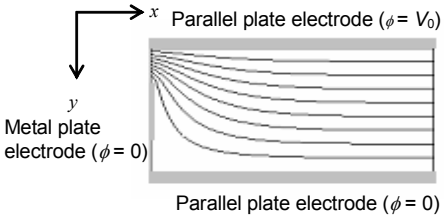

Figure 7. Potential distribution.

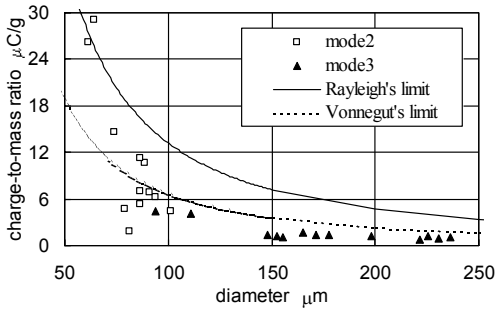

Figure 8. Critical diameter of droplet versus charge-to-mass ratio at corona discharge.

We assume that the break of the force balance between the Coulomb repulsive force and the surface tension causes the separation of droplet at the tip of the Taylor cone.[9] This condition is determined by the following Rayleigh's limit.[10]

$$q = 8\pi\sqrt{\varepsilon_0 \gamma R^3} \tag{4}$$

where ε_0 is the permittivity of free space and R is the radius of the droplet. Another model was established by Vonnegut and Neubauer based on the energy minimization principle.[11] The Vonnegut's limit is half the Rayleigh's limit. Figure 8 shows Rayleigh's and Vonnegut's limits and the measured relationship between droplet diameter and charge. Measured results were lower than Rayleigh's limit but agreed fairly well with Vonnegut's limit.

Dropping Position Control

In this electrostatic inkjet system, droplet was dispersed like mist because of repulsion of charged droplets. We constructed an experimental set-up illustrated in Fig. 9 to bundle the dispersed droplet. A ring electrode was settled between the capillary tube and the plate electrode. Figure 10 shows pictures of droplet distribution. Droplet distribution was composed of dark part and pale part as shown in Fig. 11 and 12 because small droplets were dispersed by the electrostatic repulsive force. When the voltage of the ring electrode was high, dark and pale diameters were shrunk because the electrostatic field around the tip of the tube was concentrated.

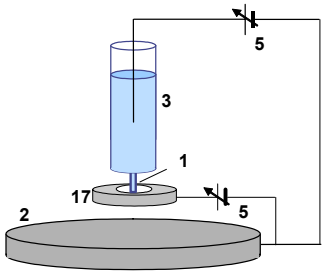

Figure 9. Experimental set-up to bundle dispersed droplet. (17: ring electrode (inner diameter: 10 mm))

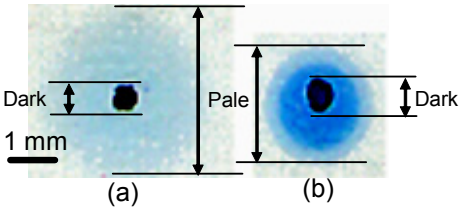

Figure 10. Picture of droplet distribution. ((a) applied voltage to water pin electrode was 3.2 kV, no control electrode, (b) applied voltage to water pin electrode was 4.9 kV, applied voltage to control electrode was 4.0 kV)

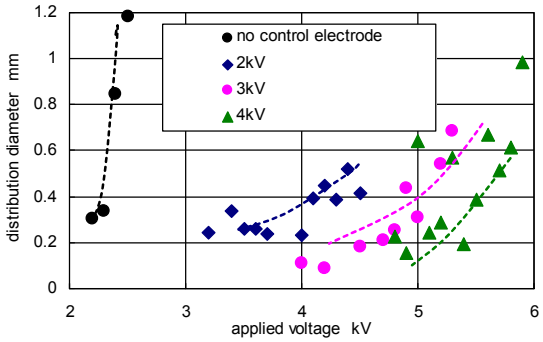

Figure 11. Distribution of dark part. (parameter: voltage of control electrode)

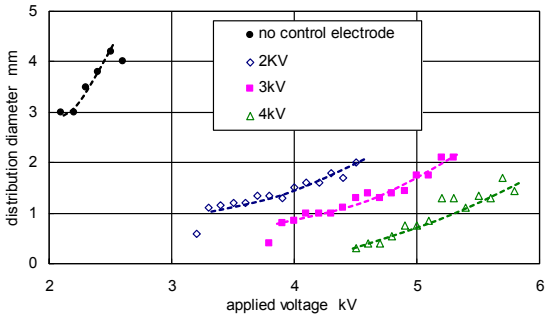

Figure 12. Distribution of pale part. (parameter: voltage of control electrode)

Concluding Remarks

We have investigated electrostatic ink jet phenomena in the gas discharge field between an insulative tube filled with ion conductive water and a plate electrode. At the beginning of corona discharge, droplets in the order of several tens of microns were dispersed like mist and the frequency of droplet formation was very high, in the order of kHz. At the stable stage of corona discharge, diameter of droplets were about one hundreds microns. Measured charge-to-mass ratio was lower than Rayleigh's limit but agreed fairly well with Vonnegut's limit.

When a ring electrode was settled between the insulative tube and the plate electrode, droplet distribution was shrunk because the electrostatic field around the tip of the tube was concentrated.

The authors would like to express their thanks to Ryosuke Nakazawa and Takashi Horikawa for their help of carrying out the experiment. This work is supported by Grant-in-Aid for Scientific Research (B), Grant-in-Aid for Young Scientists (B) and The 21st Century COE Program of Japan Society for Promotion of Science.

References

1. A. Bailey, Electrostatic Spraying of Liquids, Research Studies Press (1988) pp.60-90.
2. T. Murakami et al, High Definition Ink-jet Printing with Electrostatic Force, J. Imaging Society of Japan, 40-1 (2001) pp.40-47 (in Japanese).
3. J-D. Moon, J-G. Kim and D-H. Lee, Electrophysicochemical Characteristics of a Waterpen Corona Discharge, IEEE Trans. Industry Applications, 34-6 (1998) 1212-1217.
4. O. Yogi et al, On-Demand Droplet Spotter for Preparing Pico-to Femtoliter Droplets on Surfaces, Anal. Chem, 73 (2001) pp.1896-1902.
5. J. N. Smith, R. C. Flagan and J. L. Beauchamp, Droplet Evaporation and Discharge Dynamics in Electrospray Ionization, J. Phys. Chem, A, 106-42 (2002) pp.9957-9967.
6. H. Kawamoto, S. Umezu and R. Koizumi, Fundamental Investigation on Electrostatic Inkjet Phenomena in Pin-to-Plate Discharge System, J. Imaging Sci. & Technol., 49, 1 (2005) pp. 19-27.
7. L. Rayleigh, Phil. Mag. 14 (1882) pp.184-186.
8. H. Kawamoto, Statics of Pin Corona Charger in Electrophotography, J. Imaging Sci. Technol, 45-6 (2001) pp.556-564.
9. G. Taylor, Disintegration of water drops in an electric field, Proc. Roy. Soc. London, A 280, 383-397 (1964).
10. B. Vonnegut and R. L. Neubauer, Production of monodisperse liquid particles by electrical atomization, J. Colloid Sci, 7 (1952) pp.616-622.

Author Biography

UMEZU, Shinjiro received the BE (2001) and MS (2003) degrees in Mechanical Engineering from Waseda University, Tokyo, Japan. He is now a doctor student and a research associate in Mechanical Engineering at Waseda University, since September 2003. He awarded Best Presentation Award of the Japan Society of Mechanical Engineers in 2004. His research interests include imaging technology and MEMS technology utilizing electrostatic and gas discharge phenomena.